Electromagnetic form factor of the pion in the field-theory-inspired approach

N. N. Achasov[a*]; A. A. Kozhevnikov [a,b†]
[a] *Laboratory of Theoretical Physics, S. L. Sobolev Institute for Mathematics*
630090, Novosibirsk, Russian Federation
[b] *Novosibirsk State University*
630090, Novosibirsk, Russian Federation

Abstract

Based on the field-theory-inspired approach, a new expression for the pion form factor F_π is proposed. It takes into account the pseudoscalar meson loops $\pi^+\pi^-$ and $K\bar{K}$ and the mixing of $\rho(770)$ with heavier $\rho(1450)$ and $\rho(1700)$ resonances. The expression possesses correct analytical properties and describes the data in the wide range of the energy squared -10 GeV^2 $\leq s \leq 1$ GeV^2 without introducing the phenomenological Blatt − Weisskopf range parameter R_π. By adding the vector-pseudoscalar meson loop a good description is obtained also of the BaBaR data on the reaction $e^+e^- \to \pi^+\pi^-$ at $\sqrt{s} \leq 3$ GeV and the recent SND data on the reaction $e^+e^- \to \omega\pi^0$.

1 Introduction

The pion form factor F_π is an important characteristics of the low energy phenomena in particle physics related with the hadronic properties of the electromagnetic current in the theoretical scheme of the vector dominance model [1, 2, 3]. There are a number of expressions for this quantity used in the analysis of experimental data. The simplest approximate vector dominance model expression based on the effective $\gamma - \rho$ coupling $\propto \rho_\mu A_\mu$ [3],

$$F_\pi(s) = \frac{m_\rho^2 g_{\rho\pi\pi}/g_\rho}{m_\rho^2 - s - i\sqrt{s}\Gamma_{\rho\pi\pi}(s)}, \tag{1}$$

does not possess the correct analytical properties upon the continuation to the unphysical region $0 \leq s < 4m_\pi^2$ and further to the spacelike region $s \leq 0$, nor does it takes into account the mixing of the isovector ρ-like resonances. Since, phenomenologically [4],

$$\frac{g_{\rho\pi\pi}}{g_\rho} = 3\left(\frac{m_\rho \Gamma_{\rho\pi\pi}\Gamma_{\rho ee}}{2\alpha^2 q_\pi^3}\right)^{1/2} \approx 1.20 \tag{2}$$

the correct normalization $F_\pi(0) = 1$ is satisfied by Eq. (1) only approximately. Hereafter, $\alpha = 1/137$ stands for the fine structure constant. The formula of Gounaris and Sakurai [5] respects the above normalization condition and has the correct properties under analytical continuation. However, being based on some sort of effective radius approximation for the

*e-mail: achasov@math.nsc.ru
†e-mail: kozhev@math.nsc.ru

single $\rho(770)$ resonance, it is not suited for taking into account the mixing of $\rho(770)$ with heavier isovector mesons. The expression based on the gauge invariant $\gamma - \rho$ coupling $\propto \rho_{\mu\nu}F_{\mu\nu}$,

$$F_\pi(s) = 1 + \frac{s g_{\rho\pi\pi}/g_\rho}{m_\rho^2 - s - i\sqrt{s}\Gamma_{\rho\pi\pi}(s)}, \tag{3}$$

respect the correct normalization, but does not possesses correct analytical properties and breaks unitarity. The earlier expression [6] for F_π takes into account the strong isovector mixing, but has the shortcoming that the above normalization condition is satisfied only approximately, within the accuracy 20%.

The purpose of the present contribution is to obtain the expression for the pion form factor which possesses the correct analytical properties in the entire kinematic domain and takes into account the mixing of $\rho(770)$ with the heavier resonances $\rho(1450)$ and $\rho(1700)$.

2 Finite width effects and resonance mixing

It is known that the data on the pion form factor at energies $\sqrt{s} \geq 1$ GeV require the inclusion of heavier resonances $\rho(1450)$, $\rho(1700)$ etc. whose widths are large. The resonances are strongly mixed via their common decay modes. These effects can be taken into account in the field-theory-inspired approach based on summing to all orders of the loop corrections to the bare propagators $1/D_R^{(0)} = 1/(m_R^2 - s)$ of vector mesons. The term "bare" means that the propagators are not distorted by the mixing. The scheme can be demonstrated by taking the two-resonance mixing as an example. The effects of finite width are taken into account by introducing the diagonal polarization operator $\Pi_{RR}(s)$:

$$\frac{1}{D_R(s)} = \frac{1}{D_R^{(0)}} + \frac{1}{D_R^{(0)}}\Pi_{RR}(s)\frac{1}{D_R^{(0)}} + \frac{1}{D_R^{(0)}}\Pi_{RR}(s)\frac{1}{D_R^{(0)}}\Pi_{RR}(s)\frac{1}{D_R^{(0)}} + \cdots = \frac{1}{D_R^{(0)} - \Pi_{RR}(s)}.$$

Because of the relation

$$D_R(s) = m_R^2 - s - \mathrm{Re}\Pi_{RR}(s) - i\sqrt{s}\Gamma_R(s) \tag{4}$$

the above formula takes into account the finite width effects. The mixing is taken into account by introducing the non-diagonal polarization operator $\Pi_{RR'}(s)$:

$$\begin{aligned}
\frac{1}{D_R} &\to \frac{1}{D_R} + \frac{1}{D_R}\Pi_{RR'}\frac{1}{D_{R'}}\Pi_{RR'}\frac{1}{D_R} + \cdots = \frac{D_{R'}}{D_R D_{R'} - \Pi^2_{RR'}} \equiv \left(G^{-1}\right)_{RR}, \\
\frac{1}{D_{R'}} &\to \frac{1}{D_{R'}} + \frac{1}{D_{R'}}\Pi_{RR'}\frac{1}{D_R}\Pi_{RR'}\frac{1}{D_{R'}} + \cdots = \frac{D_R}{D_R D_{R'} - \Pi^2_{RR'}} \equiv \left(G^{-1}\right)_{R'R'}, \\
\frac{\Pi_{RR'}}{D_R D_{R'}} &\to \frac{\Pi_{RR'}}{D_R D_{R'}} + \frac{(\Pi_{RR'})^3}{(D_R D_{R'})^2} + \cdots = \frac{\Pi_{RR'}}{D_R D_{R'} - \Pi^2_{RR'}} \equiv (G^{-1})_{RR'}.
\end{aligned}$$

Here,

$$G = \begin{pmatrix} D_R & -\Pi_{RR'} \\ -\Pi_{RR'} & D_{R'} \end{pmatrix}$$

is the matrix of inverse propagators. The amplitude of the reaction is

$$A(i \to R + R' \to f) = \begin{pmatrix} g_{i\to R} & g_{i\to R'} \end{pmatrix} G^{-1} \begin{pmatrix} g_{R\to f} \\ g_{R'\to f} \end{pmatrix}.$$

The generalization to the case of arbitrary number of mixed resonances is evident.

3 Polarization operators

We take into account the analytically calculated loops of pseudoscalar (P) $\pi^+\pi^-$ and $K^+K^- + K^0\bar{K}^0$ mesons, which are diagonal in external vector mesons:

$$\Pi^{(PP)}_{\rho_i\rho_i} = g^2_{\rho_i\pi\pi}\left[\Pi^{(PP)}(s, m^2_{\rho_i}, m^2_\pi) + \frac{1}{2}\Pi^{(PP)}(s, m^2_{\rho_i}, m^2_K)\right],$$

and the vector (V)-pseudoscalar $\omega\pi^0$ and $K^*\bar{K}+\bar{K}^*K$ mesons,

$$\Pi^{(VP)}_{\rho_i\rho_i} = g^2_{\rho_i\omega\pi}\left[\Pi^{(VP)}(s, m^2_{\rho_i}, m^2_\omega, m^2_\pi) + \Pi^{(VP)}(s, m^2_{\rho_i}, m^2_{K^*}, m^2_K)\right].$$

The quark model relations among coupling constants of all vector mesons are assumed in order to express the VPP and VVP coupling constants through the $g_{\rho_i\pi\pi}$ and $g_{\omega\rho_i\pi} = g_{\rho_i\omega\pi}$ ones. Hereafter $i = 1, 2, 3, \cdots$ counts the tower of rho-like states $\rho_1 = \rho(770)$, $\rho_2 = \rho(1450)$, $\cdots$.

The diagonal polarization operators are represented in the form

$$\Pi_{\rho_i\rho_i} = \Pi^{(PP)}_{\rho_i\rho_i} + \Pi^{(VP)}_{\rho_i\rho_i}.$$

The non-diagonal ones are

$$\begin{aligned}
\Pi^{(PP)}_{\rho_1\rho_i} &= \frac{g_{\rho_i\pi\pi}}{g_{\rho_1\pi\pi}}\Pi^{(PP)}_{\rho_1\rho_1},\\
\Pi^{(PP)}_{\rho_i\rho_j} &= \frac{g_{\rho_i\pi\pi}g_{\rho_j\pi\pi}}{g^2_{\rho_1\pi\pi}}\Pi^{(PP)}_{\rho_1\rho_1},
\end{aligned}$$

$i \neq j \neq 1$, in case of the PP loop. Analogous expressions are assumed for the VP loop so that the total non-diagonal polarization operators are written as

$$\begin{aligned}
\Pi_{\rho_1\rho_i} &= \Pi^{(PP)}_{\rho_1\rho_i} + \Pi^{(VP)}_{\rho_1\rho_i},\\
\Pi_{\rho_i\rho_j} &= \Pi^{(PP)}_{\rho_i\rho_j} + \Pi^{(VP)}_{\rho_i\rho_j} + s a_{ij},
\end{aligned}$$

where a_{ij} $(i \neq j)$ are free parameters.

The quantities $\Pi^{(PP)} \equiv \Pi^{(PP)}(s, m^2_{\rho_i}, m^2_P)$ and $\Pi^{(VP)} \equiv \Pi^{(VP)}(s, m^2_{\rho_i}, m^2_V, m^2_P)$ are calculated from the dispersion relations:

$$\begin{aligned}
\frac{\Pi^{(PP)}}{s} &= \frac{1}{6\pi^2}\int_{4m_P^2}^{\infty}\frac{q^3_{PP}(s')ds'}{s'^{3/2}(s'-s-i\varepsilon)},\\
\frac{\Pi^{(VP)}}{s} &= \frac{1}{12\pi^2}\int_{(m_V+m_P)^2}^{\infty}\frac{q^3_{VP}(s')}{\sqrt{s'}(s'-s-i\varepsilon)}\left(\frac{s_0+m^2_{\rho_i}}{s_0+s'}\right)ds'.
\end{aligned} \qquad (5)$$

The factor $(s_0 + m^2_{\rho_i})/(s_0 + s')$ is introduced in order to stop a too fast growth of the $\rho_i \to VP$ decay width with the rise of the energy. Yet both integrals in Eqs. (5) are logarithmical divergent. This divergence is canceled by the subtraction of the real parts of the above equations at $s = m^2_{\rho_i}$. The result of the PP loop integration is $\Pi^{(PP)} = \Pi^{(PP)}_0 + \Pi^{(PP)}_1$, where

$$\Pi^{(PP)}_0 = \frac{s}{48\pi^2}\left[8m_P^2\left(\frac{1}{m^2_{\rho_i}} - \frac{1}{s}\right) + \left\{\begin{array}{l} v_P^3(m^2_{\rho_i})\ln\frac{1+v_P(m^2_{\rho_i})}{1+v_P(m^2_{\rho_i})},\ m_{\rho_i} > 2m_P \\ -2\bar{v}_P^3(m^2_{\rho_i})\arctan\frac{1}{\bar{v}_P},\ m_{\rho_i} \leq 2m_P \end{array}\right\}\right],$$

$$\Pi^{(PP)}_1 = \frac{s}{48\pi^2}\left\{\begin{array}{l} v_P^3(s)\left[i\pi - \ln\frac{1+v_P(s)}{1-v_P(s)}\right],\ s \geq 4m_P^2,\\ 2\bar{v}_P^3(s)\arctan\frac{1}{\bar{v}_P(s)},\ 0 \leq s < 4m_P^2,\\ -v_P^3(s)\ln\frac{v_P(s)+1}{v_P(s)-1},\ s < 0. \end{array}\right.$$

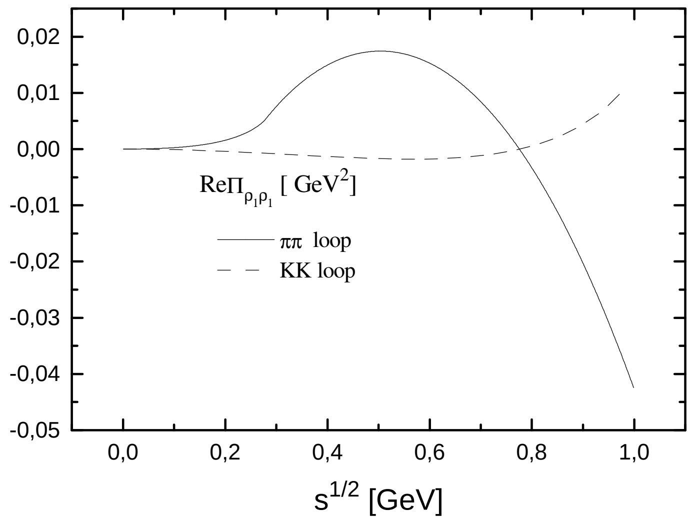

Figure 1: Energy dependence of $\mathrm{Re}\Pi_{\rho_1\rho_1}(s)$.

Here, $v_P(s) = \sqrt{1 - \frac{4m_P^2}{s}}$, $\bar{v}_P(s) = \sqrt{\frac{4m_P^2}{s} - 1}$. The plot of $\mathrm{Re}\Pi_{\rho_1\rho_1}^{(PP)}$ against $\sqrt{s}$ is shown in Fig. 1.

The result of the VP loop integration is

$$\Pi^{(VP)} = \frac{1}{48\pi^2}\left(\Pi_0^{(VP)} + \Pi_1^{(VP)} + \Pi_2^{(VP)}\right),$$

where

$$\begin{aligned}
\Pi_0^{(VP)} &= \frac{m_{\rho_i}^2 + s_0}{2s_0}\left[\frac{(m_+m_-)^3}{s_0}\left(1 - \frac{s_0}{s} - \frac{s(m_{\rho_i}^2 - s_0)}{m_{\rho_i}^4}\right)\ln\frac{m_V}{m_P} + \right. \\
&\left.\left(1 - \frac{s}{m_{\rho_i}^2}\right)m_+m_-\left(\frac{3}{2}(m_+^2 + m_-^2)\ln\frac{m_V}{m_P} + m_+m_-\right)\right] - \\
&\frac{s}{2s_0^2}\left(\frac{m_{\rho_i}^2 + s_0}{s + s_0} - 1\right)\left[(m_+^2 + s_0)(m_-^2 + s_0)\right]^{3/2}\ln\frac{\sqrt{m_+^2 + s_0} + \sqrt{m_-^2 + s_0}}{\sqrt{m_+^2 + s_0} - \sqrt{m_-^2 + s_0}}, \\
\Pi_1^{(VP)} &= -\frac{s}{m_{\rho_i}^4}\left\{\left[(m_+^2 - m_{\rho_i}^2)(m_{\rho_i}^2 - m_-^2)\right]^{3/2}\arctan\sqrt{\frac{m_{\rho_i}^2 - m_-^2}{m_+^2 - m_{\rho_i}^2}}\,\theta(m_+ - m_{\rho_i}) - \right. \\
&\left.\frac{1}{2}\left[(m_{\rho_i}^2 - m_+^2)(m_{\rho_i}^2 - m_-^2)\right]^{3/2}\ln\frac{\sqrt{m_{\rho_i}^2 - m_-^2} + \sqrt{m_{\rho_i}^2 - m_+^2}}{\sqrt{m_{\rho_i}^2 - m_-^2} - \sqrt{m_{\rho_i}^2 - m_+^2}}\,\theta(m_{\rho_i} - m_+)\right\}, \\
\Pi_2^{(VP)} &= \frac{m_{\rho_i}^2 + s_0}{s(s + s_0)}\left|(m_+^2 - s)(m_-^2 - s)\right|^{3/2}\left\{\frac{1}{2}\ln\frac{\sqrt{\frac{m_+^2 - s}{m_-^2 - s}} + 1}{\sqrt{\frac{m_+^2 - s}{m_-^2 - s}} - 1}\,\theta(m_-^2 - s) + \right. \\
&\left.\arctan\sqrt{\frac{s - m_-^2}{m_+^2 - s}}\,\theta(s - m_-^2)\theta(m_+^2 - s) + \left(i\frac{\pi}{2} - \frac{1}{2}\ln\frac{\sqrt{\frac{s - m_-^2}{s - m_+^2}} + 1}{\sqrt{\frac{s - m_-^2}{s - m_+^2}} - 1}\right)\theta(s - m_+^2)\right\}.
\end{aligned}$$

The plot of $\mathrm{Re}\Pi_{\rho_1\rho_1}^{(VP)}$ against s is shown in Fig. 2.

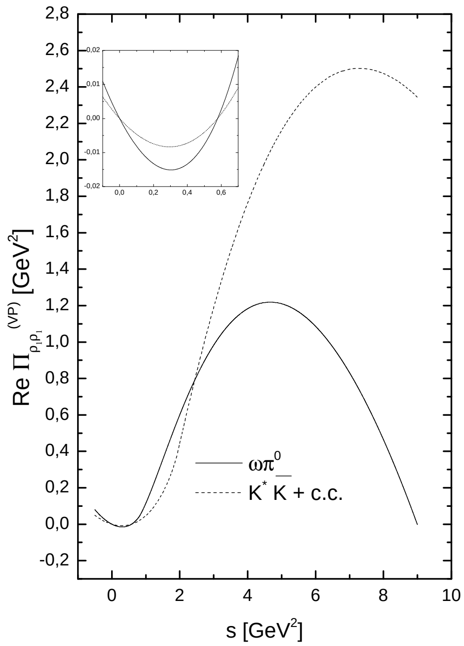

Figure 2: The dependence of $\mathrm{Re}\Pi^{(VP)}_{\rho_1\rho_1}(s)$ on energy squared. The insertion shows a smaller region $-0.2\ \mathrm{GeV}^2 \le s \le 0.8\ \mathrm{GeV}^2$.

4 Expression for the pion form factor and the measured quantities

The new expression for the pion form factor looks like

$$F_\pi(s) = (g_{\gamma\rho_1}, g_{\gamma\rho_2}, g_{\gamma\rho_3}, \cdots)G^{-1}\begin{pmatrix} g_{\rho_1\pi\pi} \\ g_{\rho_2\pi\pi} \\ g_{\rho_3\pi\pi} \\ \cdots \end{pmatrix} + \frac{g_{\gamma\omega}\Pi_{\rho_1\omega}}{D_\omega\Delta}\left(g_{11}g_{\rho_1\pi\pi} + g_{12}g_{\rho_2\pi\pi} + g_{13}g_{\rho_3\pi\pi} + \cdots\right). \tag{6}$$

The notations are as follows. $\rho_1 \equiv \rho(770)$, $\rho_2 \equiv \rho(1450)$, $\rho_3 \equiv \rho(1700)$, $\cdots$, where dots mean other possible rho-like resonances.

$$G = \begin{pmatrix} D_{\rho_1} & -\Pi_{\rho_1\rho_2} & -\Pi_{\rho_1\rho_3} & \cdots \\ -\Pi_{\rho_1\rho_2} & D_{\rho_2} & -\Pi_{\rho_2\rho_3} & \cdots \\ -\Pi_{\rho_1\rho_3} & -\Pi_{\rho_2\rho_3} & D_{\rho_3} & \cdots \\ \cdots & \cdots & \cdots & \cdots \end{pmatrix}$$

is the matrix of inverse propagators, g_{ij} are its matrix elements multiplied by $\Delta = \det G$; $g_{\gamma V} = m_V^2/g_V$ where g_V enters the leptonic partial widths like $\Gamma_{V\to e^+e^-} = 4\pi\alpha^2 m_V/3g_V^2$; $D_{\rho_i} = m_{\rho_i}^2 - s - \Pi_{\rho_i\rho_i}$. The term $\propto \Pi_{\rho_1\omega}$ takes into account the $\rho(770) - \omega(782)$ mixing. It is essential because of the mass proximity of the resonances $\rho(770)$ and $\omega(782)$. The mixings $\rho_{2,3,\cdots}$ are neglected because they are not enhanced by the effect of the mass proximity. The quantity

$$\Pi_{\rho_1\omega} = \frac{s}{m_\omega^2}\Pi'_{\rho_1\omega} + i\sqrt{s\Gamma_{\omega\pi\gamma}(s)\Gamma_{\rho\pi\gamma}(s)} \tag{7}$$

Table 1: The resonance parameters found from fitting the data SND [8], CMD-2 [9], KLOE10 [10], and the BaBaR data [11] restricted to the energies $\sqrt{s} \leq 1$ GeV.

parameter	SND	CMD-2	KLOE2010	BaBaR
m_{ρ_1} [MeV]	773.76 ± 0.21	774.70 ± 0.26	774.36 ± 0.12	773.92 ± 0.10
$g_{\rho_1 \pi\pi}$	5.798 ± 0.006	5.785 ± 0.008	5.778 ± 0.006	5.785 ± 0.004
g_{ρ_1}	5.130 ± 0.004	5.193 ± 0.006	5.242 ± 0.003	5.167 ± 0.002
m_ω [MeV]	781.76 ± 0.08	782.33 ± 0.06	782.94 ± 0.11	782.04 ± 0.10
g_ω	17.13 ± 0.30	18.43 ± 0.47	18.27 ± 0.45	17.05 ± 0.29
$10^3 \Pi'_{\rho_1\omega}$ [GeV^2]	4.00 ± 0.07	3.97 ± 0.10	3.98 ± 0.09	4.00 ± 0.06
$g_{\rho_2 \pi\pi}$	0.71 ± 0.35	0.79 ± 0.26	0.019 ± 0.004	0.21 ± 0.04
g_{ρ_2}	8.0 ± 4.4	7.6 ± 3.4	0.22 ± 0.07	4.0 ± 1.0
$g_{\rho_3 \pi\pi}$	$0.20^{+1.20}_{-0.17}$	0.76 ± 0.75	$0.055^{+0.088}_{-0.043}$	$0.011^{+0.479}_{-0.007}$
a_{23}	0.002 ± 0.011	-0.016 ± 0.057	-0.014 ± 0.040	-0.0005 ± 0.0009
$\chi^2/N_{\rm d.o.f.}$	54/35	34/19	87/65	216/260
r_π[fm]	0.635 ± 0.054	0.646 ± 0.059	0.668 ± 0.039	0.668 ± 0.053

is the polarization operator of the $\rho(770) - \omega(782)$ mixing. The real part $s\Pi'_{\rho_1\omega}/m^2_\omega$ is chosen in such a way that it vanishes at $s = 0$, and $\Pi'_{\rho_1\omega}$ is a free parameter. The inverse propagator of the $\omega(782)$ meson is

$$D_\omega = m^2_\omega - s - i\sqrt{s}\Gamma_\omega, \tag{8}$$

where the energy-dependent width $\Gamma_\omega \equiv \Gamma_\omega(s) = \Gamma_{\omega 3\pi}(s) + \Gamma_{\omega\pi\gamma}(s) + \Gamma_{\omega\eta\gamma}(s)$ includes the dominant decay mode $\omega(782) \to \pi^+\pi^-\pi^0$ and the radiative ones. The details are given in Ref. [7].

5 Comparison with existing data at -10 GeV$^2 \leq s \leq 1$ GeV^2

The new expression for F_π is compared with the measured quantities. First, we find the values of free parameters from fitting the data SND [8] CMD-2 [9], KLOE [10], and BaBaR [11] at $4m^2_\pi \leq s \leq 1$ GeV^2. One can take into account only the $\pi^+\pi^-$ and $K^+K^- + K^0\bar{K}^0$ loops in this energy region. The quantity to fit is the bare cross section

$$\sigma_{\rm bare} = \frac{8\pi\alpha^2}{3s^{5/2}}|F_\pi(s)|^2 q^3_\pi(s)\left[1 + \frac{\alpha}{\pi}a(s)\right], \tag{9}$$

$q_\pi(s) = \sqrt{s}v_\pi(s)/2$ is the momentum of the final pion, and the function $a(s)$ allows for the radiation of a photon by the final pions in the point-like approximation [12, 13, 14, 15]. The masses of the heavier vector mesons a kept fixed: $m_{\rho_2} = 1450$ MeV, $m_{\rho_3} = 1700$ MeV. The set of free parameters is m_{ρ_1}, $g_{\rho_1\pi\pi}$, g_{ρ_1}, m_ω, g_ω, $\Pi'_{\rho_1\omega}$, $g_{\rho_2\pi\pi}$, g_{ρ_2}, $g_{\rho_3\pi\pi}$, and a_{23}. Their obtained values, found from fitting the bare cross section Eq. (9), side-by-side with the corresponding χ^2 per number of degrees of freedom, are listed in Table 1 separately for the four independent measurements of SND [8], CMD-2 [9], KLOE [10], and the BaBaR data [11] restricted to the low-energy range $\sqrt{s} \leq 1$ GeV. The bottom line of this Table shows the values of the pion charge radius, $r_\pi = \sqrt{6\frac{dF_\pi(s)}{ds}}|_{s\to 0}$, calculated with the resonance parameters listed in the Table. For comparison, the averaged value of the pion charge radius cited by the PDG [4] is $r_\pi = 0.672 \pm 0.008$ fm. The corresponding curves are shown in Figs. 3, 4, and 5. We postpone the comparison with the BaBaR data until the next section.

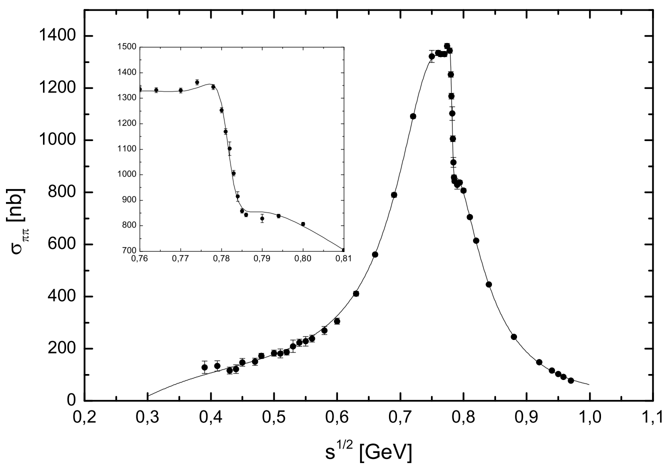

Figure 3: The results of fitting the SND data [8]. The insertion shows the $\rho\omega$ resonance region.

If one considers the energy $\sqrt{s} \sim m_{\rho(770)}$ then the treatment reduces to the case of the single $\rho(770)$ resonance whose inverse propagator is

$$D_{\rho_1} = m^2_{\rho_1} - s + (m^2_{\rho_1} - s)\frac{d\mathrm{Re}\Pi_{\rho_1\rho_1}(s)}{ds}\Big|_{s=m^2_{\rho_1}} - i\sqrt{s}\Gamma_{\rho_1\pi\pi}(s).$$

This results in the renormalization of the coupling constants $g_{\rho_1\pi\pi} \to Z_\rho^{-1/2} g_{\rho_1\pi\pi}$, $g_{\rho_1} \to Z_\rho^{1/2} g_{\rho_1}$, where

$$Z_\rho = 1 + \frac{d\mathrm{Re}\Pi_{\rho_1\rho_1}(s)}{ds}\Big|_{s=m^2_{\rho_1}} \approx 0.93,$$

and the numerical value is obtained using the entries of the Table 1. The renormalized (physical) partial widths look like

$$\Gamma_{\rho_1\pi\pi} \quad \to \quad \Gamma^{(\mathrm{phys})}_{\rho_1\pi\pi} \equiv \Gamma'_{\rho\pi\pi} = \frac{\Gamma_{\rho_1\pi\pi}}{Z_\rho},$$
$$\Gamma_{\rho_1 ee} \quad \to \quad \Gamma^{(\mathrm{phys})}_{\rho_1 ee} \equiv \Gamma'_{\rho ee} = \frac{\Gamma_{\rho_1 ee}}{Z_\rho}.$$

The Table 2 demonstrates that the renormalization brings the partial widths of the $\rho(770)$ resonance closer to the PDG values $\Gamma_{\rho\pi\pi} = 149.1 \pm 0.8$, $\Gamma_{\rho ee} = 7.04 \pm 0.06$ [4]. Note also that $\Gamma^{\mathrm{PDG}}_{\omega ee} = 0.60 \pm 0.02$ [4].

Second, using the found free parameters, we continue $F_\pi(s)$ to the space-like domain $s < 0$ and compare $|F_\pi(s)|^2$ with the data [16, 17, 18, 19]. The results are shown in Fig. 6. We emphasize that the data [16, 17, 18, 19] are not included to the fits. Hence, a good agreement, demonstrated in Figs. 3, 4, 5, 6 makes the evidence in favor of the validity of Eq. (6) for the pion form factor.

Note that the above treatment does not require the commonly accepted Blatt – Weisskopf centrifugal factor $(1 + R^2_\pi k^2_R)/(1 + R^2_\pi k^2)$, where k is the pion momentum, in the expression for $\Gamma_{\rho\pi\pi}(s)$ [4]. The fact is that the usage of R_π dependent centrifugal barrier penetration factor

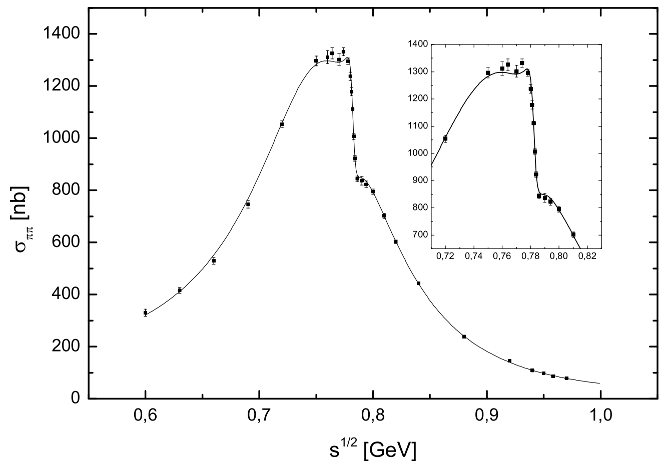

Figure 4: The same as in Fig. 3 but for the CMD-2 data [9].

Table 2: The renormalization constant and the partial widths of the $\rho(770)$ and $\omega(782)$ calculated with the parameters of the Table 1.

	SND	CMD-2	KLOE2010	BaBaR
Z_ρ	0.9273 ± 0.0003	0.9277 ± 0.0002	0.9279 ± 0.0002	0.9277 ± 0.0001
$\Gamma_{\rho\pi\pi}$	139.93 ± 0.29	139.54 ± 0.39	139.12 ± 0.29	139.34 ± 0.19
$\Gamma'_{\rho\pi\pi}$	150.90 ± 0.31	150.42 ± 0.42	149.92 ± 0.31	150.20 ± 0.20
$\Gamma_{\rho ee}$	6.56 ± 0.01	6.41 ± 0.01	6.29 ± 0.01	6.47 ± 0.01
$\Gamma'_{\rho ee}$	7.07 ± 0.01	6.91 ± 0.01	6.78 ± 0.01	6.97 ± 0.01
$\Gamma_{\omega ee}$	0.59 ± 0.02	0.51 ± 0.03	0.52 ± 0.03	0.60 ± 0.02

in particle physics (for example, in the case of the $\rho(770)$ meson [4]), results in the problem which is overlooked. Indeed, the meaning of R_π is that this quantity is the characteristic of the potential (or the t-channel exchange in field theory) resulting in the phase $\delta_{\rm bg}$ of the potential scattering in addition to the resonance phase [20]. For example, in case of the P-wave scattering in the potential $U(r) = G\delta(r - R_\pi)$ where the resonance scattering is possible, the background phase is $\delta_{\rm bg} = -R_\pi k + \arctan(R_\pi k)$. At the usual value of $R_\pi \sim 1$ fm, $\delta_{\rm bg}$ is not small. However, in the ρ meson region, the background phase shift $\delta_{\rm bg}$ is negligible and the phase shift δ_1^1 is completely determined by the resonance. See Fig. 7, where shown are the phase δ_1^1 calculated with the parameters from the BaBaR column of the table 1 and the data points from Refs. [21, 22] is presented. Therefore, the descriptions of the hadronic resonance distributions taking into account the parameter R_π have a dubious character.

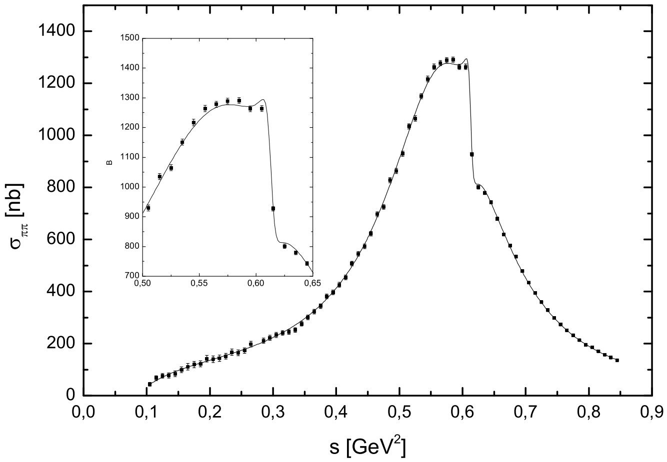

Figure 5: The same as in Fig. 3 but for the KLOE-2100 data [10].

6 Reactions $e^+e^- \to \pi^+\pi^-$ and $e^+e^- \to \omega\pi^0$ at energies up to 3 GeV

When going to the energies higher than 1 GeV one should take into account the $\omega\pi$ and $K^*\bar{K} + \bar{K}^*K$ loops in the polarization operators. This somehow takes into account the multi-particle intermediate states. To this end we undertake the joint fit of the BaBaR data [11] on the reaction $e^+e^- \to \pi^+\pi^-$ at energies $\sqrt{s} \le 3$ GeV, and the SND data on the reaction $e^+e^- \to \omega\pi^0$ at energies $\sqrt{s} < 2$ GeV [23, 24]:

$$\sigma_{e^+e^-\to\omega\pi^0} = \frac{4\pi\alpha^2}{3s^{3/2}} \left|A_{e^+e^-\to\omega\pi^0}\right|^2 q^3_{\omega\pi},$$

$$A_{e^+e^-\to\omega\pi^0} = (g_{\gamma\rho_1}, g_{\gamma\rho_2}, g_{\gamma\rho_3}, \cdots)G^{-1} \begin{pmatrix} g_{\rho_1\omega\pi} \\ g_{\rho_2\omega\pi} \\ g_{\rho_3\omega\pi} \\ \cdots \end{pmatrix}$$

Fitting with $\rho(770) + \rho(1450) + \rho(1700)$ does not permit the joint description of the cross section of the reactions $e^+e^- \to \pi^+\pi^-$ and $e^+e^- \to \omega\pi^0$. We undertake the fit with four rho-like resonances $\rho(770) + \rho(1450) + \rho(1700) + \rho(2100)$. Their masses, coupling constants are free except the condition

$$\frac{g_{\rho_1\pi\pi}}{g_{\rho_1}} + \frac{g_{\rho_2\pi\pi}}{g_{\rho_2}} + \frac{g_{\rho_3\pi\pi}}{g_{\rho_3}} + \frac{g_{\rho_4\pi\pi}}{g_{\rho_4}} = 1$$

necessary for correct normalization $F_\pi(0) = 1$. Some of the fitted parameters are: $m_{\rho_1} = 765.55 \pm 0.09$ MeV, $g_{\rho_1\pi\pi} = 6.117 \pm 0.003$, $g_{\rho_1} = 4.830 \pm 0.002$, $m_\omega = 781.95 \pm 0.09$ MeV, $\Pi'_{\rho_1\omega} \times 10^3 = 3.98 \pm 0.07$ GeV^2, $m_{\rho_2} = 1362 \pm 3$ MeV, $m_{\rho_3} = 1503 \pm 8$ MeV, $m_{\rho_4} = 1960 \pm 6$ MeV. The results of this joint fit are shown in Figs. 8 and 9. Note that taking into account the VP loop in the pion form factor results in unwanted singularities at $s < -0.4$ GeV^2. These

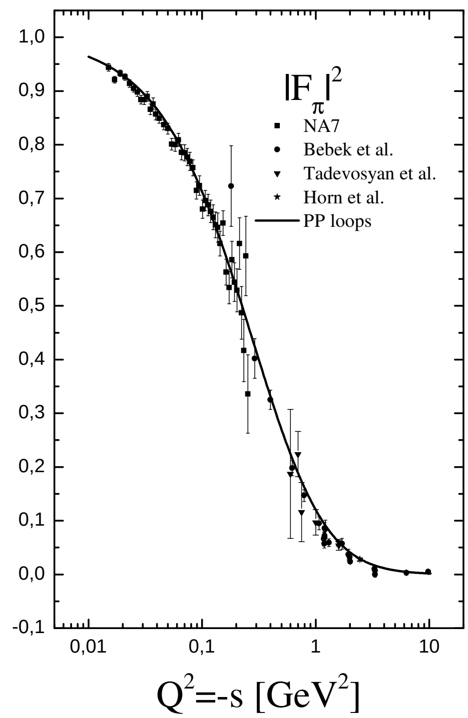

Figure 6: The pion form factor squared in the space-like region $s < 0$ evaluated using the resonance parameters of the Table 1, the BaBaR column. The experimental data are: NA7 [16], Bebek *et al.* [17], Horn *et al.* [18], Tadevosyan *et al.*[19].

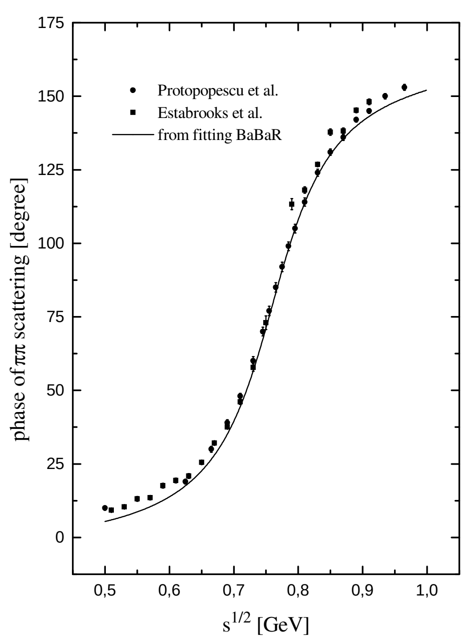

Figure 7: The phase shift δ_1^1 of $\pi\pi$ scattering. The data are, respectively, Protopopescu et al. [21] and Estabrooks et al. [22]. The curves corresponding to the parameters obtained from fitting the SND, CMD-2, and KLOE data are not shown because they coincide with the curve evaluated using the parameters from the fit of the BaBaR data, shown here.

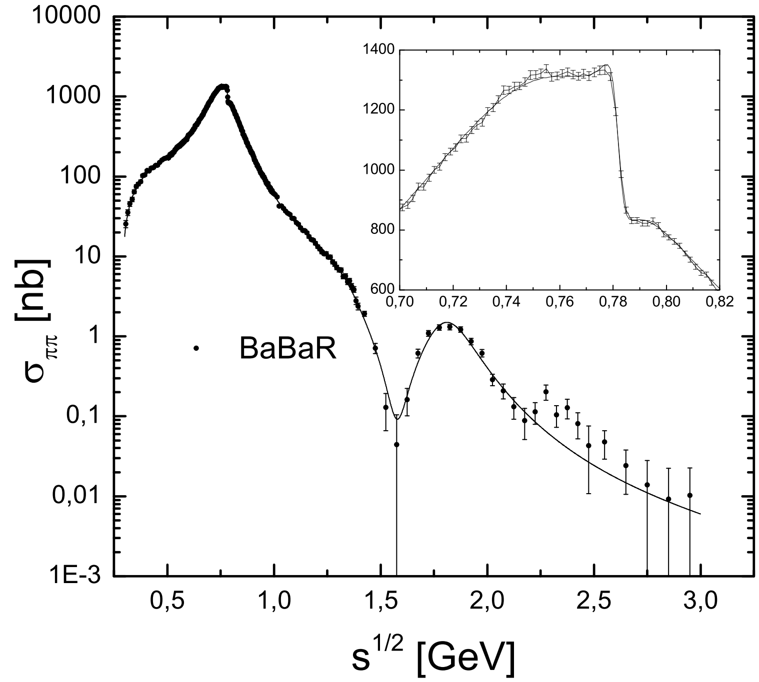

Figure 8: The same as in Fig. 3, but for the BaBaR data [11].

may be attributed to the way of slowing down the growth of $\Gamma_{\rho\to\omega}(s)$ with growing s in the time-like region which is chosen here in the simplest form $(s_0 + m_V^2)/(s_0 + s)$. The problem demands an additional study.

7 Conclusion

To conclude, the new expression, Eq. (6), for the pion form factor $F_\pi(s)$ is obtained which gives a good description of the data of SND, CMD-2, KLOE, BaBaR on $\pi^+\pi^-$ production in e^+e^- annihilation at $\sqrt{s} < 1$ GeV, describes the scattering kinematical domain, and does not contradict the data on $\pi\pi$ scattering phase δ_1^1. The preliminary treatment shows that the joint description of the cross section of the reactions $e^+e^- \to \pi^+\pi^-$ and $e^+e^- \to \omega\pi^0$ is possible upon taking into account the vector – pseudoscalar loops. Going to higher energies demands the inclusion of the axial-vector – pseudoscalar loops. This work is now at progress.

We are grateful to the Organizers of QUARKS-2012 Seminar for invitation to participate and the pleasant and stimulating atmosphere. The partial support from Russian Foundation for Basic Research Grant no. RFFI-10-02-00016 and the Interdisciplinary project No 102 of Siberian Division of Russian Academy of Sciences is acknowledged.

References

[1] J. J. Sakurai. Ann. Phys. (N.Y) **11**, 1 (1960).

[2] M. Gell-Mann and F. Zachariasen. Phys. Rev. **124**, 953 (1961).

[3] N. M. Kroll, T. D. Lee, and B. Zumino. Phys. Rev. **157**, 1376 (1967).

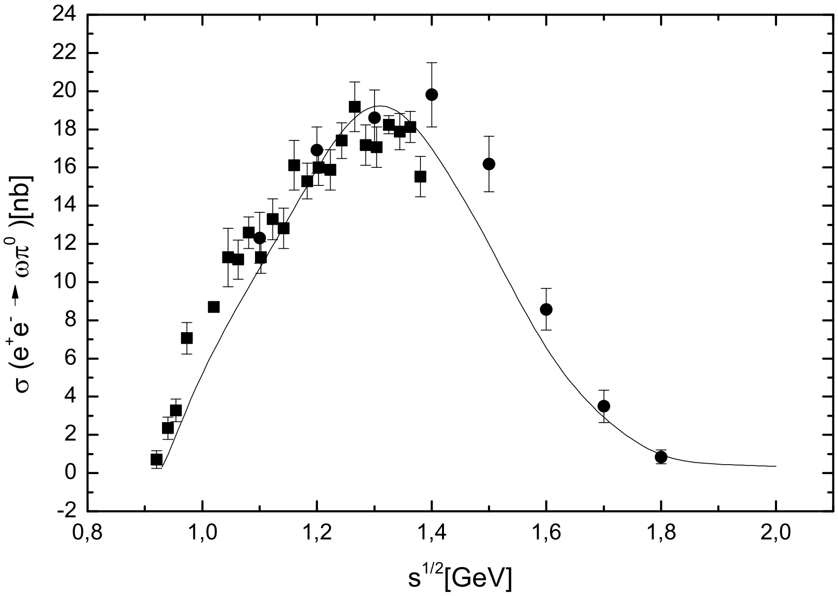

Figure 9: Fitting the SND data [23, 24].

[4] J. Beringer, *et al.* (Particle Data Group), Phys. Rev. D**86**, 010001 (2012).

[5] G. J. Gounaris and J. J. Sakurai. Phys.Rev.Lett. **21**, 244 (1968).

[6] N. N. Achasov and A. A. Kozhevnikov. Phys.Rev.D**55**, 2663 (1997) [arXiv:hep-ph/9609216v1].

[7] N. N. Achasov and A. A. Kozhevnikov. Phys.Rev.D**83**, 113005 (2011) [arXiv:1104.4225].

[8] M. N. Achasov, *et al.*. J.Exp.Theor.Phys. **101**, 1053 (2005); Zh.Eksp.Teor.Fiz. **101**, 1201 (2005) [arXiv:hep-ex/0506076v1].

[9] R. R. Akhmetshin, *et al.* (CMD-2 Collaboration), Phys.Lett.B**648**, 28 (2007) [arXiv:hep-ex/0610021v3].

[10] F. Ambrosino, *et al.* (KLOE Collaboration), Phys.Lett. B**700**, 102 (2011)[arXiv:1006.5313].

[11] B. Aubert, *et al.* (The *BABAR* Collaboration), Phys.Rev.Lett.**103**, 231801 (2009) [arXiv:0908.3589v1].

[12] J. S. Schwinger. *Particles, Sources and Fields. Volume II*, (Addison-Wesley Publishing Company, Reading, MA, 1973).

[13] M. Deers and K. Hikasa. Phys. Lett. B**252**, 127 (1990).

[14] K. Melnikov. Int. Journ. Mod. Phys. A**16**, 4591 (2001).

[15] A. Hoefer, J. Gluza, and F. Jegerlehner. Eur. Phys. Journ. C**24**, 51 (2002).

[16] S. R. Amendolia, *et al.* Nucl.Phys.B**277**, 168 (1986).

[17] C. J. Bebek, *et al.* Phys.Rev.D**17**, 1693 (1978).

[18] T. Horn, *et al.* Phys.Rev.Lett.**97**,, 192001 (2006).

[19] V. Tadevosyan, *et al.* Phys.Rev.C**75**, 055205 (2007).

[20] J. M. Blatt and V. F. Weisskopf. *Theoretical Nuclear Physics,* (Wiley, New-York – London, 1952).

[21] S. D. Protopopescu, *et al.* Phys. Rev. D**7**, 1279 (1973).

[22] P. Estabrooks and A. D. Martin. Nucl. Phys. B**79**, 301 (1974).

[23] M. N. Achasov, *et. al.* Phys.Lett.B**486**,29(2000).

[24] M. N. Achasov, *et. al.* Pisma ZhETP.**94**,796(2011).